



SHADING IMPACT ANALYSIS FOR A HOUSEHOLD PV SYSTEM IN A DISTRIBUTED GRID

Amit Kumar Suman

EEE Department, Katihar Engineering College, Katihar

Vikash Kumar

EEE Department, Rashtrakavi Ramdhari Singh Dinkar College of Engineering, Begusarai

Abstract: This research introduces a simplified method for modeling and analyzing the performance of partially shaded photovoltaic modules. The method utilizes the shading ratio as a key parameter. This approach incorporates the attributes of shaded area and shadow opacity into the model of the solar cell. The methodology under investigation aims to enhance the characterization of shaded photovoltaic systems by outlining a systematic approach to measure and quantify the influence of shadows. Moreover, utilizing image processing techniques, the examination of the shading ratio yields a collection of principles that are valuable in forecasting the current-voltage characteristics and the maximum power points of shaded solar modules. The relationship between the shading ratio and shading patterns can aid in the monitoring real solar installations. The experimental results confirm the effectiveness of the suggested method in both monocrystalline as well as polycrystalline solar panel technologies.

Keywords: partial shading; photo-generated current; photovoltaic performance; maximum power point; image processing

1. Introduction

Photovoltaic (PV) system integration into electrical grids is becoming more common as an attractive replacement for distributed-energy resource. Because of their ease of installation and adaptability, they have been integrated into both urban and rural electricity systems. However, shadows cast by nearby structures interfere with PV installations, resulting in power losses and problems with structural integrity. As a result, many researchers have created techniques for modeling to further comprehend the effects of shadows on PV systems [1]. Although these contributions are significant, the observed behavior and detrimental situations indicate the necessity to enhance the quantification of shadow influence. Undoubtedly, novel modeling and supervision methodologies are necessary to enhance comprehension and mitigate the occurrence of production losses in photovoltaic (PV) systems. Furthermore, the implementation of inventive methodologies can enhance the configuration of power converters and control strategies, thereby mitigating the adverse effects caused by shadows. Consequently, the creation of new techniques to measure and monitor the influence of shadows is now a crucial concern for enhancing the efficiency of

photovoltaic systems.

The aforementioned research topic is based on the reverse-bias characteristics of shaded photovoltaic cells. Bishop proposed a widely accepted model for understanding the behavior of shaded PV-cells under reverse-bias conditions [2]. Quaschnig et al. expanded upon Bishop's concept by introducing the two-diodes model. Kawamura et al. conducted a simulation of the bishop model, taking into account shadow transmittance, to investigate the corresponding I-V characteristics. Guo et al. examined the impact of changing shadows on the PV-power characteristics to enhance the model's dynamism. Subsequently, Olalla et al. conducted simulations of extensive photovoltaic (PV) systems with a high level of detail, utilizing diffuse irradiance to accurately represent the impact of partial shading. Furthermore, Díaz et al. introduced a comprehensive and streamlined model that takes into account the geometry of shadows.

Silvestre et al. expand the bishop model to examine PV module performance in the shade ratio study [3]. Three important parameters and the photo-current for a variable shading ratio were included in the mathematical model that Jung et al. presented for the output characteristics of a photovoltaic module. By employing a partial shading technique with two distinct shading ratios, Yong et al. describe a non-disruptive cell-level evaluation of a solar module that extracts the shunt resistances and the short-circuit currents of individual cells. He investigates hotspot problems in a photovoltaic module with varying numbers of PV cells by employing multiple shading ratio situations. In order to examine the impact of the shadow rate on the most crucial PV module characteristics, the work provided in creates a simulation and modeling of PV modules' performance under partial shadowing for multiple shadow rates testing individual cells in PV modules [4].

As demonstrated by this brief historical overview, the researchers have over time developed more detailed and comprehensive methodologies to describe the behavior of shaded PV systems and the impact of the shading ratio [5]. However, given the changing nature of shadows in real-world applications, research on evolutionary PV installations now necessitates precise but simplified analysis.

Within this particular framework, our research suggests an enhanced conceptualization of the shadowing ratio and a novel experimental configuration for incorporating the shadow characteristics into the shaded PV model [6]. This endeavor entails the evaluation of the shading ratio in order to quantify the impact of shadows on PV installations. The shading ratio is a relationship between the shading factor and the shadow characteristics of the obscured area. In addition, by utilizing image processing techniques, the proposed method incorporates an innovative experimental configuration for monitoring and analyzing the shadow effect via the shading ratio. A set of principles to estimate the current–voltage function of shaded solar panels is generated by this analysis. Furthermore, the correlation observed between the shading ratio and the shadow image patterns facilitated the development of a simplified expression for the purpose of localizing the maximum power points (MPPs) under real-world shaded circumstances. In conclusion, experimental validation of these correlations establishes the groundwork for the implementation of image processing techniques to quantify and monitor the shadow impact on PV installations [7]. The methodology that employs the coloration ratio and image processing.

The structure of this document is as follows. Section 2 provides an overview of the modeling

background. Section 3 outlines the recommended methodology. The analysis in Section 4 focuses on simulations of shaded PV modules. Section 5 provides a comprehensive explanation of the experimental setup used to validate and correlate the proposed method with shadow image patterns. Ultimately, the experimental findings are analyzed and examined.

2. Photovoltaic Model for Shaded Conditions

Shaded photovoltaic (PV) modules provide a significant risk of experiencing issues with structure and a high possibility of reduced power generation. Many researchers have conducted research on this behavior specifically focusing on PV-cells [8]. The approach offered by Bishop from the proposed models has demonstrated a satisfactory level of consistency with controlled tests. Nevertheless, the intricate characteristics of the shading phenomenon have highlighted the necessity of supplementing these methods. This section provides an overview of the characteristics and modeling techniques used to characterize the behavior of shaded photovoltaic (PV) systems.

2.1. Shaded PV Modules and Modeling Background

The study employs a conventional configuration with partial shading, as depicted under clear weather conditions. The temperature in the surrounding environment was 15 °C, while the intensity of solar radiation on a flat surface was 910 W/m² at 1:00 p.m. The experimental results depicted demonstrate the significant influence on the I–V and P–V curves. Partial shadows can result in the emergence of several maximum power points (MPPs) [9]. Furthermore, research has demonstrated that these partial shadows can result in excessive heat buildup and the occurrence of hot-spot problems.

This shading behavior has been explored by several authors. Based on prior work on the avalanche breakdown theory, Bishop develops a model for the reverse-bias properties of shaded solar cells. The authors present a numerical simulation in order to examine the I–V characteristic in the shadow [10]. The study proposed an alternate model for different types of PV cells. The referenced paper discusses PV performance with regard to shadow rate. It investigates thermal stability and hotspot dangers [11]. The work is an outline of a study of the influence of shadow movement. A discrete I–V model for shaded PV installations is proposed.

Previous research has established a correlation between the influence of shading and the generation of power from photovoltaic systems. The authors in Ref. [12] address the topic of shadowed photovoltaic (PV) installations in urban settings through the utilization of 3D modeling. Ref. [13] introduces a streamlined approach for modeling the power output of photovoltaic systems affected by shading. Nevertheless, the intricate characteristics of the shading phenomenon indicate that the suggested methods can be expanded upon to enhance the performance of the PV module. Initially, this part provides a description of Bishop's model for shaded PV-cells.

1.1. Shaded PV-Cell Model

This section outlines the suggested methodology for modeling shaded photovoltaic (PV)

cells in PV modules, taking into consideration the fine level of detail and the potential to scale up to larger PV systems [14]. Under conditions of reduced illumination, the photovoltaic cells can be compelled to conduct current in the opposite direction of their normal operation, known as reverse bias [15]. Consequently, the PV-cell terminals experience a negative voltage, resulting in a severe surge of reverse current. Bishop elucidates the phenomenon of current multiplication by employing which represents the shaded PV-cells with a non-linear multiplier factor.

The relationship between the PV-cell currents I and the PV-cell voltage V_c is represented by Equation (1). Here R_s denotes the series resistance due to conductive losses and R_p denotes the shunt resistance due to dispersed losses inside the p-n material. V_t is the thermal voltage, while I_0 is the inverse saturation current. k is the fraction of current involved in avalanche breakdown, V_b is the breakdown voltage, and n is the avalanche breakdown exponent in the nonlinear multiplier factor. The photo-generated current, I_{ph} .

The PV cell function can be adequately described by the model put forth by Bishop under fully unshaded as well as shaded situations [16]. Nevertheless, this model fails to account for the geometric and optical characteristics of partial shadows, potentially resulting in a substantial reduction in precision. In fact, the photo-generated current is dependent on uniform irradiance, and Bishop does not address partial shading in Ref. Certain authors have expanded the parameters of this model to incorporate shadow characteristics. Due to the complexity of shadows, experimental approaches to quantify these properties are less prevalent in the scientific literature [17]. The subsequent section explains the suggested methodology for computing partially shaded photovoltaic modules, taking into account measurable shadow properties [18].

3. Proposed Approach for Partially Shaded PV Modules

The preceding section outlined a prevalent methodology for modeling shaded PV modules. Nevertheless, empirical findings have demonstrated that this method can experience a compromise in precision when confronted with real-world scenarios including partial shading [18]. In account of the intricate characteristics of the shading phenomenon, it is necessary to incorporate the shadow properties into the shadow analysis while ensuring that the computational effort remains constant owing to the scalability of PV systems [19]. The aforementioned considerations inspired the development of the suggested strategy in this section.

3.1. Partially Shaded PV-Cell Model

Figure 3 illustrates that within a photovoltaic (PV) module, the partially shaded cells exhibit two prominent shadow characteristics. The first characteristic is the representation of shadow geometry by $a_s + a_i = 1$,

where,

a_s = the fraction of shaded cell area

a_i = the fraction of illuminated cell area.

The optical characteristics of the solar irradiance on the PV module, denoted by the shadow transmittance τ and the shading factor S_f , are included in the second shadow feature.

$$\tau = G_s/G_i$$

G_s = scattered irradiance on the shadow

G_i = incident irradiance

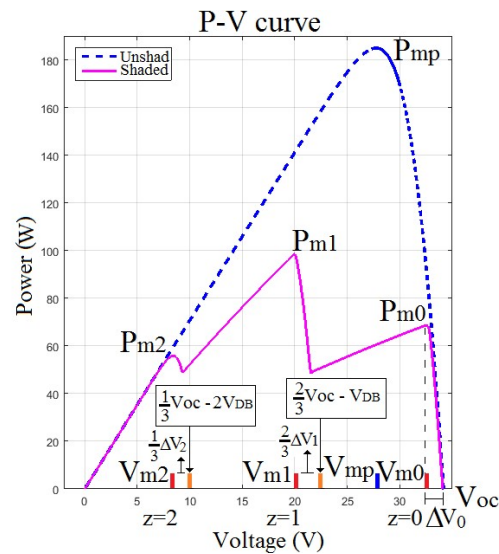
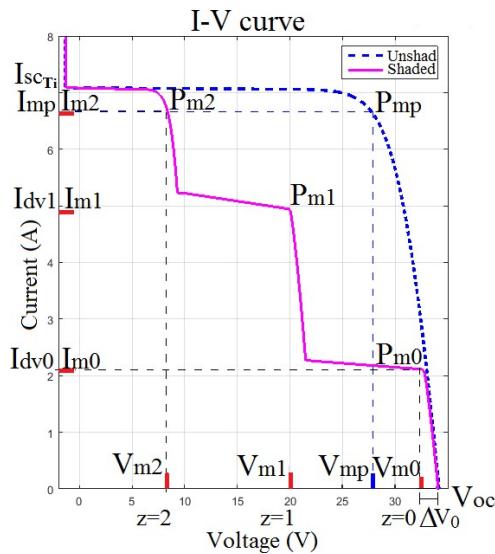
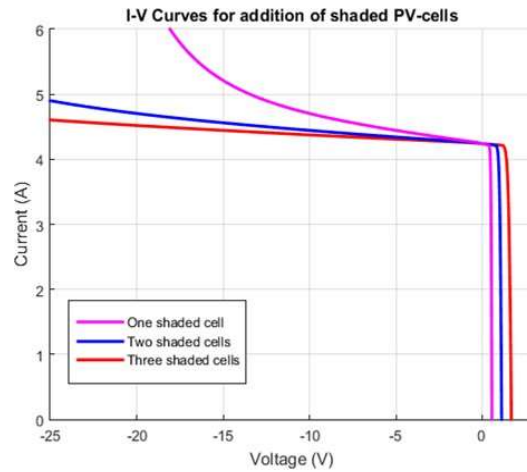
A value of $\tau = 0$ indicates that all of the incident irradiance is obstructed within the region under consideration. On the other hand, when $\tau = 1$, it indicates that all the available irradiance shines on the considered region as the scattered irradiance G_s becomes equal to G_i . The shading factor S_f , which characterizes the opacity of shadows.

3.2 Influence of the Shading Ratio δ on the PV Module Behavior

This section connects the previous proposed approach with shadow patterns in order to extend the shadow impact analysis at the PV module level [20]. PV modules are formed by series connections of PV-cells, and PV module manufacture typically links by-pass diodes to groups of PV-cells to reduce damage risk. Thus, the voltage in a PV module V_p with m groups of q PV-cells and by-pass diode voltage V_{BD} .

Parameter	Values		
z	0	1	2
δ	0.28	0.7	1.0
Group	G3	G2	G1
P approx. (W)	64.09	95.02	53.65
P Simul. (W)	68.06	98.39	55.27
Rel. error	0.06	0.03	0.03

Table 1. Maximum power points—Case: diagonal shadow



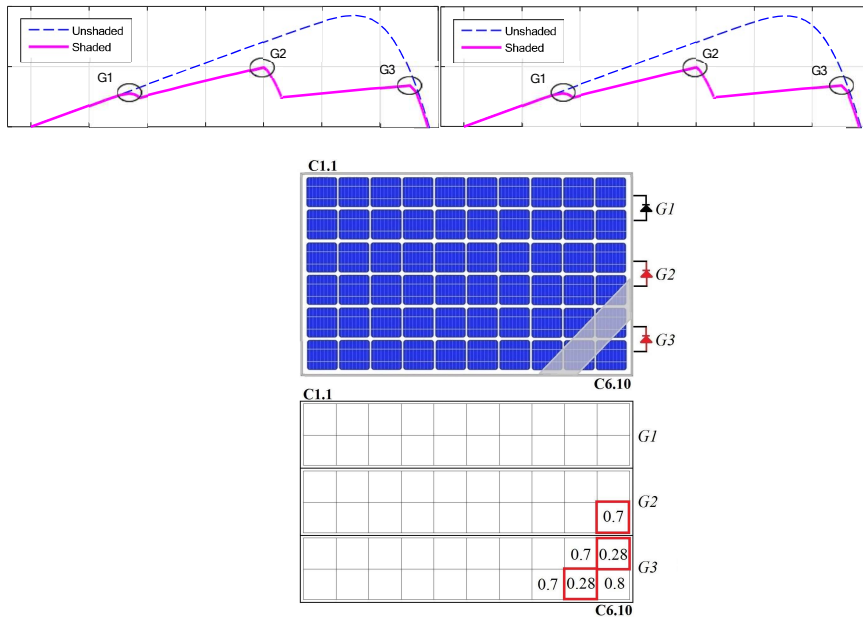
4. Simulation Analysis of Shaded PV Modules

The shadow pattern scenarios in this section have been chosen to demonstrate the potential aspects of proposed simulation methodologies. First, two scenarios demonstrate the influence of single shaded cells distributed throughout numerous groups and shaded cells grouped into a single group. Then, two scenarios are shown to demonstrate the impact of shadow movement. The last simulation aims to generate a shaded PV string [21]. The simulations were carried out on a standard computational platform by solving using the lineaments. Furthermore, the simulated shading ratios are specified for further research and correlation with experimental patterns. The shaded PV-module images in this section are purely for illustration purposes and do not represent any specific software.

4.1. Simulation of Partially Shaded PV Modules

The nominal parameters of the simulated PV modules are $I_{sc} = 8.3A$ and $V_{oc} = 37.3 V$ with simulation conditions of incident irradiance $G_i = 850 W/m^2$ and cell temperature $T_c = 45 ^\circ C$. The cases consider a uniform shading factor $S_f = 0.8$. We also consider a conventional PV

module with sixty cells distributed in groups of twenty cells connected to by-pass diodes [3]. The analysis uses a matrix notation ij where δ_{ij} represents the shading ratio of a PV-cell in the relative position ij in a PV module. The first case depicted in Figure 9 shows all groups with a single shaded cell. This simulation is intended to study the impact of single shaded cells in the normal current–voltage behavior. In Figure 9, the PV module current I_{PV} is normalized in ratio to $I_{sc}T_i = 7.1$ A. Therefore, on the y-axis, the $I_{Norm} = I_{PV}/I_{sc}T_i$. This simulation case shows that the lowest divergence current I_{dv} is proportional to the shaded cells with the lowest value of δ . For instance, the first divergence current I_{dv0} in Figure 9b is caused by the PV-cell with $\delta_{2,10} = 0.20$ of group one. Figure 9 confirms that the divergence current I_{dvz} due to each group is close to $I_{dvz} = \delta_z I_{sc}T_i$, where δ_z depends on the shaded cell C_{ij} with the lowest value of δ in the group.



○ **Simulation of Partially Shaded PV String**

Figure 13 depicts the final studied case at level of PV string. To facilitate understanding, this figure highlights the most significant shaded PV cells in an irregular shadow pattern. The simulations results allow identifying four regions. The region R_1 depends on $G1.2$ and $G2.2$. In this region, PV1 $\delta_{3,1}$ and PV2 $\delta_{4,1}$ cause the lowest I_{dv0} in the PV string. R_1 is extended by around 20V because the bypass activation of two groups. $G1.1$ and $G1.3$ produce region R_2 . The divergence current I_{dv1} in R_2 is proportional to the 40% of $I_{sc}T_i$, which is caused by PV1 $\delta_{1,1} = \delta_{2,1} = \delta_{5,1} = \delta_{6,1} = 0.4$. Region R_3 is produced by $G3.2$ with the single PV-cell PV3 $\delta_{3,1} = 0.6$. The bypass activation points and the I–V curve slope are higher in region R_3 ; therefore, this single cell is more vulnerable to dissipating power and generating hot-spots (see Figure 6b). Finally, R_4 depends on the unshaded PV groups and provides the highest MPP of all regions.

Type	Monocrystalline		Polycrystalline	
	Case 1	Case 2	Case 3	Case 4
G_i	820 W/m ²	910 W/m ²	710 W/m ²	540 W/m ²
T_C	31 °C	31 °C	31 °C	30 °C
I_{ph}	7.07 A	7.85 A	6.14 A	4.67 A
I_{dv}	2.16 A	2.7 A	1.33 A	1.66 A
α_i	0.98	0.91	0.97	0.90
δ_i	0.31	0.34	0.22	0.36
S_f	0.70	0.72	0.8	0.71

Table 3. Shading factor results for the PV modules under testing

4.2. Identified Patterns between the Shading Ratio and the PV Module Behavior

The following findings highlight the patterns identified from the interaction between the shading ratio and the partial shadows.

1. The divergence currents I_{dvz} are proportional to the lowest shading ratio δ_z in each shaded PV group. Thus, $I_{dvz} \approx \delta_z I_{sc} T_i$ for $\delta_z < 1$.
2. Shaded cells have a minimal impact on the I–V curve if their shading ratio is greater than the lowest shading ratio in the same group.
3. In a group, shaded cells with shading ratios close to the lowest shading ratio have a lower overheating risk because the reverse bias voltage is distributed between them.

5. Experimental Validation and Discussion

This section outlines the experimental configuration used to verify the analysis put out in Section 3. Furthermore, this section presents a methodological approach to measure the shading ratio through the utilization of image processing techniques. The analysis of experimental findings is provided.

5.1. Test for Partially Shaded PV Modules

Two shadow situations are taken into consideration in the designed experiments. Moreover, the tests compare two widely used commercial technologies using monocrystalline and polycrystalline PV modules.

5.2. Discussion of Results

Under the assumption of a uniform S_f , the findings additionally indicate that the I–V curve is not significantly impacted by the smaller shaded cell areas when compared to the larger shaded cell areas within the same group. The PV-cells C3.7 and C5.8 from example 1-monocrystalline have a negligible effect on the I-V characteristics. Shaded cells with small shaded areas, on the other hand, can affect the I-V curve if they have the smallest shaded area in the group. For example, the PV-cell C4.12 in Case 2-polycrystalline can affect the I-V curve.

Figure 3 demonstrates that PV-cells that are shaded and have shading ratios close to the lowest shading coefficient in the group exhibit I-V curves with reduced slopes due to the characteristics of the reverse-bias voltage. Specifically, PV-cells C5.12 and C6.10 in Case 2-polycrystalline exhibit a shallower slope compared to PV-cell C4.12 in Case 2-polycrystalline. Hence, PV-cell C4.12 carries a higher likelihood of power dissipation. It provides the slopes for both case 2-monocrystalline and case 2-polycrystalline. These cases include a single shaded cell within a group. The data shown in indicate a little mismatch in the monocrystalline situation, but a more substantial difference in the polycrystalline case. The authors have conducted a comprehensive experimental investigation on partial shade and slope detection.

The mean squared error (MSE) of model validation in Table 11 also indicates an insignificant mismatch between case 1 and case 2 in both technologies. Various reasons, such as alterations in internal parameters, current route, or leakage currents, can account for this discrepancy. Indeed, certain authors have demonstrated that the series and shunt resistances are influenced by the irradiance circumstances. Soto et al. propose that the series resistance is influenced by the level of irradiance, as it declines at lower irradiance levels and can even become negative. Prior studies also demonstrate the presence of negative values for the series resistance when exposed to low levels of irradiation. In reference [21], the series resistance and the shadow rate both exhibit an increase, resulting in an amplified power dissipation by the series resistance. However, the majority of publications regard these differences as less significant. They treat the series resistance as independent of the incident irradiance and temperature, and achieve satisfactory precision. On the other hand, the analysis of the shunt resistances under low irradiance settings has been extensively recorded in literature due to the significant effect of the reverse-bias conditions.

The results demonstrate the use of image processing techniques with the suggested models to quickly identify the global maximum power points (MPPs). The estimated maximum power points (MPPs) for monocrystalline and polycrystalline examples are determined respectively. The resulting values are then recorded. These data clearly demonstrate the relationship between the lowest shading ratios and the MPP computation. The aforementioned attributes of streamlined and rapid localization of MPPs offer potential for integration into existing image recognition-based power generation supervision techniques.

Furthermore, the methodology proposed in this section may be beneficial to image processing-based supervision strategies by taking into account the following findings regarding shaded areas:

- The divergence currents are generated by the shaded cells in each group with the greatest shaded area.
- Shaded cells slightly alter the operation point set by the PV cell with the largest shaded area.
- The presence of localized shadows on individual shaded cells within a cluster can intensify the risk due to overheating.
- When multiple cells of the same group cast uniform shadows, structural hazards are reduced.
- The MPPs can be swiftly localized by taking into account the shaded PV-cells with the

most shaded regions in each group.

Comparison with Other Approaches

The contributions given in this research are compared to current techniques in the literature in this section presents methodologies that address PV modeling challenges from various angles. The reverse-bias behavior is described in utilizing a nonlinear multiplication factor connected with the shunt resistance current. The influence of partial shadows, on the other hand, is not addressed. To ensure convergence, the second approach provides a discrete strategy. This study proposes a generalized method for simulating the electrical behavior of PV installations by discretizing currents and voltages in PV systems, which is mostly based on bishop modeling. Quantification methods for shadow parameters, on the other hand, are outside the scope of this work. The authors incorporate forecasting tools for PV energy generation. The PV installation is characterized at the single-cell level with high resolution, and the unexpected influence of small-area shadows is estimated. The authors emphasize the importance of miniature shadows in power generation. However, the structural condition is not included.

This methodology aims to create a high-speed computational technique for simulating shaded photovoltaic (PV) modules. This research examines the performance of PV modules when PV cells are connected in parallel and series under the same external conditions. The analysis is conducted using the Brune method. Nevertheless, this approach fails to consider the impact of the reverse-bias characteristics. The shaded photovoltaic (PV) behavior is described by the authors using the two-diodes model. Using real-time simulator data, the accuracy of the modeling technique is verified and compared to that of the neural network approach and the single-diode model. Nonetheless, this method fails to consider the effects of partially shaded PV cells. The methodology outlined provides a streamlined and precise expression for MPPs on the level of multiple strings. In order to simulate the PV array, an improved iteration of the single-diode model is utilized, which is then explicitly reformulated using the Lambert W function. On the other hand, the irradiance is regarded uniform on shaded PV groups.

In contrast with prior methods, the distinguishing feature of our work is the development and investigation of a methodology for quantifying a ratio capable of describing shaded behavior without adding computational complexity. Furthermore, the suggested methodology gives a helpful expression for determining MPPs quickly using image processing techniques and unshaded parameters. However, the proposed method might be enhanced by investigating additional PV-cell parameters and employing image recognition methods to estimate non-uniform shading effects.

6. Conclusions

This research introduced an alternative method to explain the characteristics of partially shadowed photovoltaic (PV) modules. The proposed approach provided a precise and improved definition of the shading ratio δ . The strategy under investigation outlined a methodology capable of empirically quantifying the shadow features and the shading ratio δ . Moreover, the examination of the findings enabled us to determine the correlation between the shadow patterns and alterations in I–V and P–V features. An expedited

formula was devised to efficiently compute MPPs by utilizing the minimum shading ratio in each group and the standard operational parameters. The testing findings confirmed the effectiveness of the suggested method in both monocrystalline and polycrystalline technologies. Additional examination should take into account non-uniform shading variables and other aspects of the photovoltaic (PV) cell, such as the series and shunt resistances. In future research, it is recommended to develop a supervision technique by including image-processing algorithms into the monitoring of output power in photovoltaic (PV) installations.

References

1. Toledo, O.M.; Filho, D.O.; Diniz, A.S.A.C.; Martins, J.H.; Vale, M.H.M. Methodology for evaluation of grid-tie connection of distributed energy resources - Case study with photovoltaic and energy storage. *IEEE Trans. Power Syst.* **2013**, *28*, 1132–1139.
2. Brooks, A.E.; Cormode, D.; Cronin, A.D.; Kam-Lum, E. PV system power loss and module damage due to partial shade and bypass diode failure depend on cell behavior in reverse bias. In Proceedings of the 2015 IEEE 42nd Photovoltaic Specialist Conference (PVSC), New Orleans, LA, USA, 14–19 June 2015; pp. 1–6.
3. Bressan, M.; Basri, Y.E.; Galeano, A.; Alonso, C. A shadow fault detection method based on the standard error analysis of I–V curves. *Renew. Energy* **2016**, *99*, 1181–1190.
4. Batzelis, E.; Georgilakis, P.; Papathanassiou, S. Energy models for photovoltaic systems under partial shading conditions: A comprehensive review. *IET Renew. Power Gener.* **2015**, *9*, 340–349.
5. Jena, D.; Ramana, V.V. Modeling of photovoltaic system for uniform and non-uniform irradiance: A critical review. *Renew. Sustain. Energy Rev.* **2015**, *52*, 400–417.
6. MacAlpine, S.; Deline, C.; Erickson, R.; Brandemuehl, M. Module mismatch loss and recoverable power in unshaded PV installations. In Proceedings of the 2012 38th IEEE Photovoltaic Specialists Conference, Austin, TX, USA, 3–8 June 2012; pp. 1388–1392.
7. Hidalgo-Gonzalez, P.L.; Brooks, A.E.; Kopp, E.S.; Lonij, V.P.; Cronin, A.D. String-Level (kW-scale) IV curves from different module types under partial shade. In Proceedings of the 2012 38th IEEE Photovoltaic Specialists Conference, Austin, TX, USA, 3–8 June 2012; pp. 1442–1447.
8. Daliento, S.; Chouder, A.; Guerriero, P.; Pavan, A.M.; Mellit, A.; Moeini, R.; Tricoli, P. Monitoring, Diagnosis, and Power Forecasting for Photovoltaic Fields: A Review. *Int. J. Photoenergy* **2017**, *2017*, 13.
9. Bai, J.; Cao, Y.; Hao, Y.; Zhang, Z.; Liu, S.; Cao, F. Characteristic output of PV systems under partial shading or mismatch conditions. *Sol. Energy* **2015**, *112*, 41–54.
10. Zhao, Q.; Shao, S.; Lu, L.; Liu, X.; Zhu, H. A New PV Array Fault Diagnosis Method Using Fuzzy C-Mean Clustering and Fuzzy Membership Algorithm. *Energies* **2018**, *11*, 238.
11. Lahouar, F.E.; Hamouda, M.; Slama, J.B.H. Design and control of a grid-tied three-phase three-level diode clamped single-stage photovoltaic converter. In Proceedings of the 2015 Tenth International Conference on Ecological Vehicles and Renewable Energies

- (EVER), Monte Carlo, Monaco, 31 March–2 April 2015; pp. 1–7.
12. Golroodbari, S.Z.M.; de Waal, A.C.; van Sark, W.G.J.H.M. Improvement of Shade Resilience in Photovoltaic Modules Using Buck Converters in a Smart Module Architecture. *Energies* **2018**, *11*, 250.
 13. Triki-Lahiani, A.; Abdelghani, A.B.B.; Slama-Belkhodja, I. Fault detection and monitoring systems for photovoltaic installations: A review. *Renew. Sustain. Energy Rev.* **2017**, doi: 10.1016/j.rser.2017.09.101.
 14. Madeti, S.R.; Singh, S. A comprehensive study on different types of faults and detection techniques for solar photovoltaic system. *Sol. Energy* **2017**, *158*, 161–185.
 15. Bishop, J. Computer simulation of the effects of electrical mismatches in photovoltaic cell interconnection circuits. *Sol. Cells* **1988**, *25*, 73–89.
 16. Quaschnig, V.; Hanitsch, R. Numerical simulation of current–voltage characteristics of photovoltaic systems with shaded solar cells. *Sol. Energy* **1996**, *56*, 513–520.
 17. Kawamura, H.; Naka, K.; Yonekura, N.; Yamanaka, S.; Kawamura, H.; Ohno, H.; Naito, K. Simulation of I–V characteristics of a PV module with shaded PV cells. *Sol. Energy Mater. Sol. Cells* **2003**, *75*, 613–621.
 18. Guo, S.; Walsh, T.M.; Aberle, A.G.; Peters, M. Analysing partial shading of PV modules by circuit modelling. In Proceedings of the 2012 38th IEEE Photovoltaic Specialists Conference, Austin, TX, USA, 3–8 June 2012; pp. 2957–2960.
 19. Olalla, C.; Clement, D.; Choi, B.S.; Maksimovic, D. A branch and bound algorithm for high-granularity PV simulations with power limited SubMICs. In Proceedings of the 2013 IEEE 14th Workshop on Control and Modeling for Power Electronics (COMPEL), Salt Lake City, UT, USA, 23–26 June 2013; pp. 1–6.
 20. Díaz-Dorado, E.; Cidrás, J.; Carrillo, C. Discrete I–V model for partially shaded PV-arrays. *Sol. Energy* **2014**, *103*, 96–107.
 21. Silvestre, S.; Chouder, A. Effects of shadowing on photovoltaic module performance. *Prog. Photovolt. Res. Appl.* **2008**, *16*, 141–149.